JOURNAL OF NATURAL PRODUCTS

Article

pubs.acs.org/jnp

The Thermal and Enzymatic Taxifolin−Alphitonin Rearrangement

Paul W. Elsinghorst,*[,†,§] Taner Cavlar,[†] Anna Müller,[†] Annett Braune,[‡] Michael Blaut,[‡] and Michael Gütschow[†]

[†]Pharmaceutical Chemistry I, Pharmaceutical Institute, University of Bonn, 53121 Bonn, Germany

[§]Central Institute of the Bundeswehr Medical Service Munich, 85748 Garching-Hochbrück, Germany

[‡]Department of Gastrointestinal Microbiology, German Institute of Human Nutrition Potsdam-Rehbruecke, 14558 Nuthetal, Germany

ABSTRACT: This report describes a detailed investigation of the thermal and enzymatic conversion of taxifolin to alphitonin. Chromatographic separation of the four dihydroquercetin stereoisomers **1**−**4** in combination with circular dichroism spectroscopy permitted elucidation of the kinetics of this rearrangement and characterization of the different reaction pathways involved. Our findings are corroborated by quantum chemistry calculations that reveal a unique cascade of tautomerization processes leading from taxifolin to alphitonin and also explain the racemization of alphitonin at room temperature. Furthermore, the substrate specificity toward (+)-taxifolin of an enzyme from *Eubacterium ramulus* catalyzing this intriguing rearrangement is demonstrated.

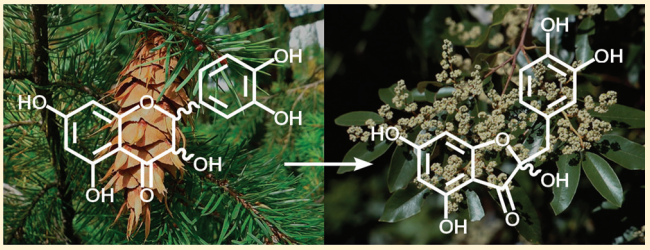

Polyphenols exhibit several positive effects on human health, e.g., antioxidant, antimicrobial, antiviral, and antitumor activities. A variety of health-promoting products containing polyphenols are now available in the market as dietary supplements.[1,2] These polyphenols either are absorbed in the human intestine in their original form or may be subject to microbial metabolism.[3,4] The two polyphenols in focus of this report are taxifolin and alphitonin, with the former representing a 4-chromanone, i.e., a dihydroflavonol, and the latter a 3(2*H*)-benzofuranone, i.e., an auronol. While dihydroflavonols are found in many plant families, auronols are much more limited in their abundance and are especially present in Rhamnaceae. Both classes of compounds usually occur as glycosides, and notable auronol representatives are alphitonin, maesopsin, amaronols A and B, zeyherin, marsuposide, and hovetrichoside.[5−13] Alphitonin was isolated first in 1922 from the wood of *Alphitonia excelsa*, a common Australian tree.[5,14] Taxifolin, also referred to as dihydroquercetin, was named after the Douglas fir, *Pseudotsuga taxifolia*, from which it was isolated first.[15] It has been recognized as a constituent of heartwood and needles in Pinaceae, where it contributes to resistance against fungi and termites.[15−18] Both compounds are tightly linked to each other by (i) a thermal and (ii) an enzyme-catalyzed rearrangement reaction.

The observation that auronols can be obtained by treatment of dihydroflavonols with alkali[19,20] was further generalized in 1995 by Kiehlmann et al., who obtained alphitonin by heating a neutral, aqueous solution of taxifolin for several hours, although an oxidative side reaction occurred producing quercetin.[19−21] Ohmura et al. corroborated this observation by detecting alphitonin after steaming of taxifolin-containing wood.[18] Hence, steaming of wood, a common procedure in timber production, or hot extraction of wood might lead to formation of auronols, e.g., alphitonin, that were not present in the original material. However, the occurrence of alphitonin in the heartwood of *A. excelsa* was affirmed, as it was also detected after cold extraction.[5] Recently, investigations of the intestinal metabolism of quercetin revealed that the human gut bacterium *Eubacterium ramulus* transforms quercetin to taxifolin and subsequently to alphitonin.[22] The same metabolites were observed with the human colonic microbiota.[23] Since quercetin, mainly as glycosides, is abundant in food and beverages, alphitonin deserves particular attention with respect to formation, further transformation, and biological activity. The proposed mechanism of the thermal taxifolin−alphitonin rearrangement is outlined in Scheme 1, with special attention to the possible dihydroquercetin stereoisomers.[16,18,19,21,22]

The determination of the absolute configuration of the four dihydroquercetin stereoisomers and of some of its glycosides has been the subject of several attempts. The corresponding assignments were based on experimental results from optical rotary dispersion and circular dichroism (CD) measurements, and specifications of the absolute configuration rely either on a comparison with the data of (+)-catechin or on theoretical considerations.[16,24−33] The CD spectra reported by Nonaka et al.[28] were used as the reference for the computational studies of this report.

To investigate the thermal and enzymatic taxifolin−alphitonin rearrangement, we established a chromatographic system to separate all four dihydroquercetin stereoisomers. Quantum chemical calculations were performed to assign their conformations and to analyze the racemization process and the

Received: July 31, 2011
Published: October 12, 2011

Scheme 1. Proposed Route of the Rearrangement of Dihydroquercetins (1−4) to Alphitonin (8) via the Quinone Methides 5, the Chalcone 6, and the Diketone 7

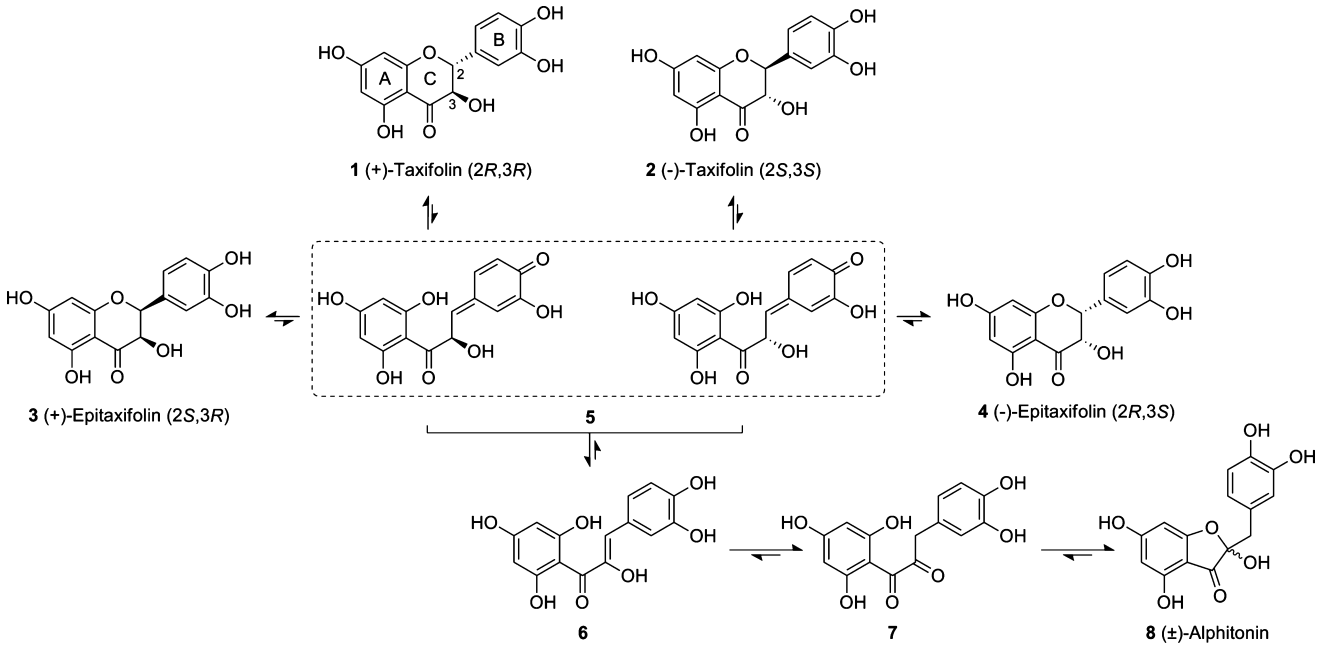

limiting energy barriers. The enzymatic conversion of taxifolin to alphitonin was characterized with respect to its substrate specificity and kinetic profile.

RESULTS AND DISCUSSION

Our initial attempts were directed toward the design of a suitable reaction system to investigate the thermal taxifolin−alphitonin rearrangement above 100 °C over a 14-day period. To minimize oxidative quercetin formation, a reaction setup was devised as follows. Taxifolin was placed in an amber glass vial under argon, and oxygen-free water was added. The vial was submersed in a solution of gallic acid as an external protection from oxidation. The mixture was heated at 115 °C in an oil bath, and aliquots were removed and subjected to reversed-phase HPLC analysis.

Baseline separation of the four dihydroquercetin stereoisomers and alphitonin was achieved with an established chromatographic system. Using cellulose tris(4-methylbenzoate) as the chiral stationary phase, all analytes were separated with sufficient resolution and plate numbers (Figure 1A, Table 1). In addition, CD spectra were recorded for each peak and the absolute configuration of the four dihydroquercetin stereoisomers was assigned on the basis of the work of Nonaka et al.[28] However, during thermal conversion of (+)-(2*R*,3*R*)-taxifolin (**1**), the temporary enrichment of one epitaxifolin enantiomer was observed. While the formation of one epitaxifolin enantiomer **4** would result only from a keto−enol tautomerization within the C ring,[32] formation of the other epitaxifolin enantiomer **3** would require ring-opening to a quinone methide and recyclization (Scheme 1). Therefore, we expected the temporarily accumulating epitaxifolin enantiomer to be (−)-(2*R*,3*S*)-epitaxifolin (**4**). However, the observed CD Cotton effect at 298 nm was positive, whereas literature assignments require a negative Cotton effect for (−)-(2*R*,3*S*)-epitaxifolin (**4**) at this wavelength. At this point, we were prompted to perform quantum chemical calculations using the ORCA computational package considering further literature[34] for the prediction of the CD spectra of (−)-(2*R*,3*S*)-epitaxifolin (**4**) and (−)-(2*S*,3*S*)-taxifolin (**2**). Both diastereomers were subjected to potential energy surface (PES) scans at the B3LYP/TZVP computational level applying the COSMO model in methanol and varying the two conformational processes, i.e., a C-ring flip leading to equatorial/axial inversion (φ_1 = C6−C7−C8−O9) and a full rotation of the B−C-ring bond (φ_2 = O9−C8−C10−C11) (Figure 2A,B). From these PES scans, local minima that are significantly populated at ambient temperature (energy cutoff 3 kcal/mol) were identified according to Boltzmann statistics and further optimized (Table 2). Finally, CD spectra of these minima were retrieved by a TDDFT/B3LYP/TZVP approach and weighted according to their individual Boltzmann population derived from energies at the RI-SCS-MP2/TZVP computational level (Figure 2D). The CD spectra obtained by these quantum chemical calculations were in good agreement with the reported literature spectra. Thus, our preliminary assumption of a fast keto−enol tautomerism within the C ring was proven to be wrong. The configuration of the temporarily enriched epitaxifolin is 2*S*,3*R* (compound **3**), and it is formed by C-2 epimerization.[21,35]

Whereas the separation of the four dihydroquercetin stereoisomers was successfully achieved, several attempts to separate the two putative alphitonin enantiomers by chiral HPLC analysis failed, even with applying different HPLC gradients and modifying the temperature. We also performed chiral electrokinetic chromatography, where the alphitonin peak again remained unresolved (Figure 1C). To explain this observation, a fast on-column racemization was considered and investigated in detail. Alphitonin racemization was assumed to proceed by ring-opening to the diketone **7**, being in a keto−enol equilibrium with the α-hydroxychalcone **6** (Scheme 1). To prove this assumption, an NMR experiment involving deuterium incorporation at the benzylic position of alphitonin was envisaged, as it had been successfully applied in an equilibrium study of a related benzofuranone.[6] Thus, a sample of alphitonin obtained by thermal conversion was dissolved in

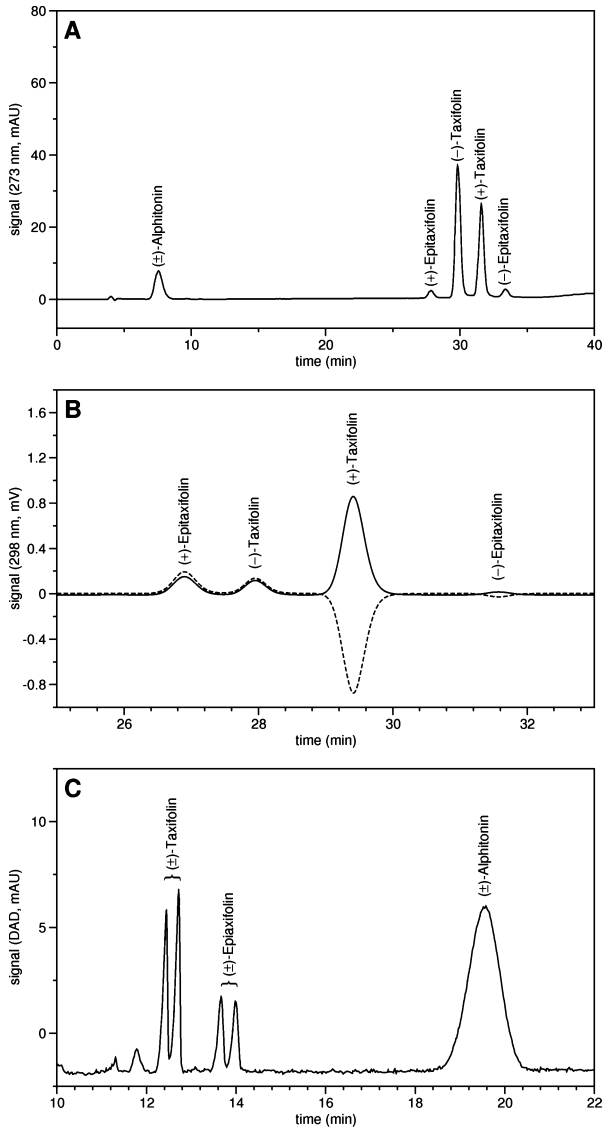

Figure 1. (A) Chiral separation of the dihydroquercetin stereoisomers and alphitonin by RP-HPLC. The chromatogram was recorded in the course of the thermal conversion of racemic (±)-taxifolin to alphitonin. (B) Online CD detection coupled to chiral RP-HPLC. The chromatogram was recorded in the course of the thermal conversion of enantiopure (+)-taxifolin to alphitonin. (C) Chiral electrokinetic chromatography of the dihydroquercetin stereoisomers and alphitonin. The chromatogram was recorded in the course of the thermal conversion of racemic (±)-taxifolin to alphitonin.

Table 1. Chromatographic Parameters of the Four Dihydroquercetin Stereoisomers

compound	retention time (min)	theoretical plates	resolution to following peak (min)
(+)-epitaxifolin (**3**)	27.9	20300	2.6
(−)-taxifolin (**2**)	29.9	25600	2.4
(+)-taxifolin (**1**)	31.6	31100	2.4
(−)-epitaxifolin (**4**)	33.4	33800	

D_2O, and the H/D exchange was followed by subsequent NMR recordings. However, even after one week at room temperature, no exchange of the benzylic protons was observed, in contrast to the complete exchange of all phenolic and even of all A-ring

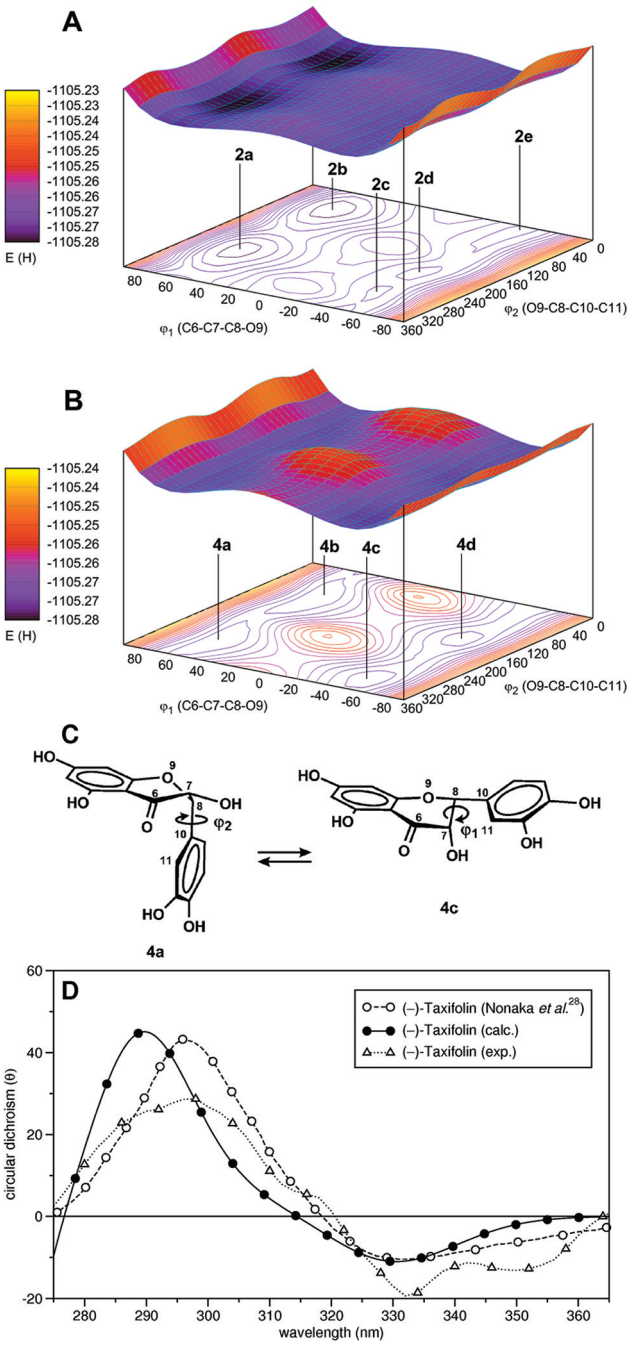

Figure 2. Potential energy surface (PES) scans of (−)-taxifolin (A) and (−)-epitaxifolin (B) to simulate (i) a C-ring flip leading to equatorial/axial inversion (φ_1 = C6−C7−C8−O9) and (ii) a full rotation of the B−C-ring connecting bond (φ_2 = O9−C8−C10−C11). Local minima are indicated in the contour plots (see also Table 2). (C) Selected stereoconformers of (−)-epitaxifolin with denoted dihedral angles φ_1 and φ_2. (D) The predicted CD spectra (shown here for (−)-taxifolin) are in good agreement with experimental observations and corroborate the reported stereochemical assignments.[28]

protons (5.8−5.9 ppm), the latter being exchanged due to keto−enol tautomerism (Figure 3A).[36] Concerning the keto−enol tautomerism of **6** and **7**, this result did not support the postulated **8** ⇌ **7** ⇌ **6** equilibrium (Scheme 1) and was also in disagreement with literature reports of keto−enol tautomerism in maesopsin.[6,37]

dx.doi.org/10.1021/np200639s | J. Nat. Prod. 2011, 74, 2243−2249

Table 2. Local Minima from Conformational Analysis of (−)-Taxifolin (2) and (−)-Epitaxifolin (4)[a]

conformer	type	φ_1 (deg)	φ_2 (deg)	N_i (%)
2a	equatorial	57.0	236.5	41.31
2b	equatorial	57.1	58.8	56.68
2c	axial	−51.8	306.7	0.74
2d	axial	−48.8	199.6	0.63
2e	axial	−49.2	12.4	0.63
4a	axial	51.9	282.0	18.52
4b	axial	54.4	75.1	32.61
4c	equatorial	−53.7	315.4	27.32
4d	equatorial	−54.0	138.2	21.54

[a]Data were obtained at the B3LYP/TZVP level of theory applying a COSMO model in methanol. φ_1 refers to the dihedral angle C6−C7−C8−O9 (C-ring flip) and φ_2 to O9−C8−C10−C11 (B−C-ring bond rotation). N_i is the corresponding Boltzmann population used for weighting of CD spectra.

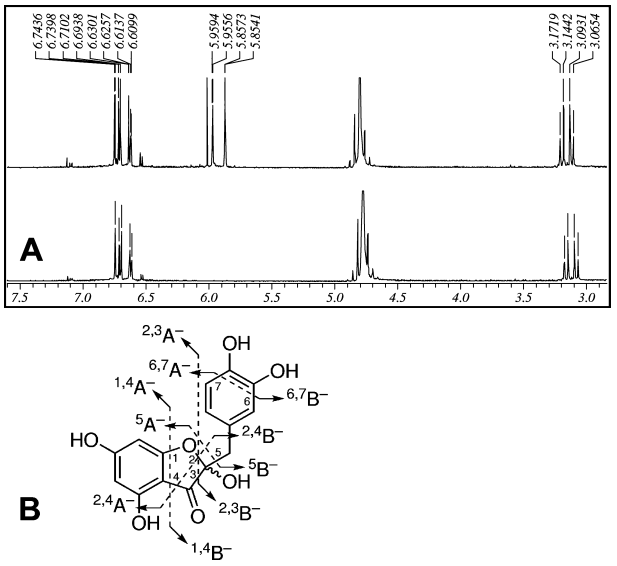

Figure 3. (A) ^{1}H NMR spectra of alphitonin immediately after dissolving (top) and after one week of incubation (bottom) in D_2O. (B) MS fragmentation of alphitonin (see also Experimental Section).

To reconfirm the auronol structure of **8**, MS analysis was performed and corroborated its cyclic, and thus chiral, benzofuranone structure (Figure 3B; see also Experimental Section). Once again, we applied quantum chemical calculations to gain further insight into the equilibrium processes connecting the two alphitonin enantiomers to each other and to the four dihydroquercetin stereoisomers.

Using the ORCA program suite, minimum energy conformers were optimized for **2**, the assumed intermediates **5**−**7**, and **8** at the B3LYP/TZVP level of theory applying a COSMO water model, followed by frequency calculations at 25 and 115 °C. The obtained Gibbs free energies confirmed the obvious assumption that ring-opening of taxifolin to quinone methide **5** is the most energy-consuming step (Figure 4). Boltzmann statistics predicted a final alphitonin−taxifolin equilibrium ratio of 92:8, which is in excellent agreement with the experimental result of a nearly complete conversion (Figure 6A,B). Furthermore, the Gibbs free energies of **6**−**8** provided a convincing explanation for the racemization without deuterium incorporation, as the equilibrium populations are 76.8% for alphitonin (**8**), 23.0% for the diketone **7**, and only 0.2% for the

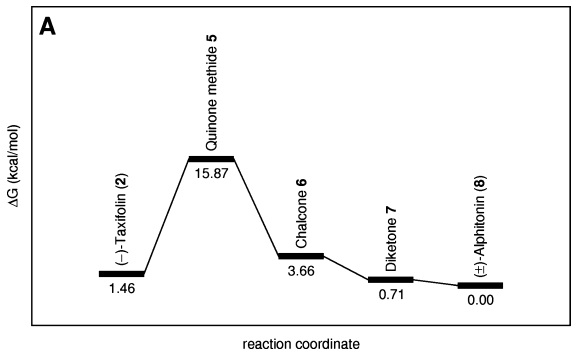

Figure 4. Quantum chemistry calculations for the interconversion of **2** to **8** reveal the ring-opening to the intermediate quinone methide **5** as the energy barrier for the taxifolin−alphitonin rearrangement.

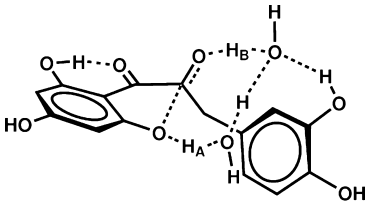

9

Figure 5. Transition state **9** involving two water molecules was found to facilitate racemization of alphitonin (**8**) via diketone **7**.

chalcone **6**. Using the Gaussian program suite[38] at the B3LYP/6-311G++(df,pd) computational level, the transition state **9** connecting **7** and **8** was investigated taking a possible proton relay by one or two water molecules into consideration (Figure 5; Table 3).[39] The transition state involving two water molecules represents an energy barrier that can be readily overcome at room temperature (2.34 kcal/mol), and thus, alphitonin (**8**) may racemize at room temperature via the intermediate diketone **7**. This result is in accordance with the observation that auronols are usually obtained as racemates but can be resolved after derivatization of the hemiacetal hydroxy group.[40−42] However, as the existence of α-hydroxychalcone **6** is very short-lived, practically no deuterium is incorporated during racemization in D_2O.

Chiral chromatographic analysis of the in-process control samples taken during thermal and enzymatic conversion revealed a first-order mechanism for the taxifolin−alphitonin rearrangement (Figure 6A,B). A pronounced enantioselectivity toward (+)-taxifolin was observed for the enzyme from *E. ramulus* accompanied by a high turnover rate, which was 200-fold accelerated at room temperature in the presence of 1.9 μg protein/mL of the partially purified enzyme ($k = 7.26 \times 10^{-4}$ s^{-1}, Figure 6B) when compared to thermal conversion at 115 °C ($k = 3.60 \times 10^{-6}$ s^{-1}, Figure 6A). Due to the observed fast racemization of alphitonin, no conclusions could be drawn on stereoselective product formation. The further characterization of the enzyme from *E. ramulus* will be the subject of future work. Aurone derivatives exhibit a notable therapeutic potential, e.g., as antiviral, immunosuppressive, and chemopreventive agents or as inhibitors of multidrug resistance.[43−47] The thermal and enzymatic conversion reported herein will be useful to provide alphitonin for future biological evaluation.

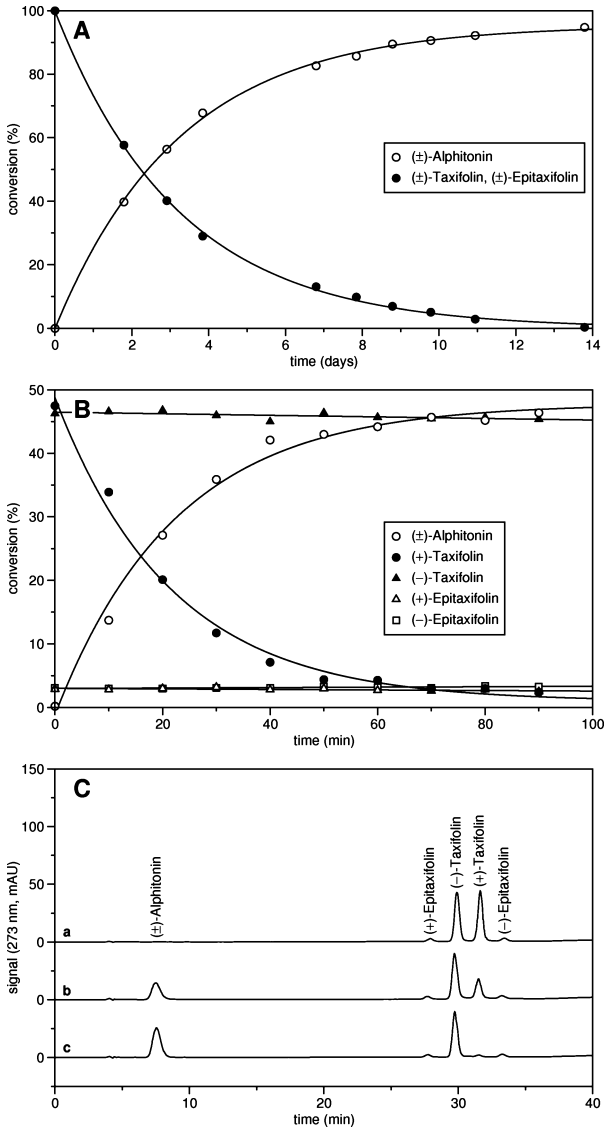

Figure 6. (A) Kinetic analysis of the thermal taxifolin–alphitonin rearrangement at 115 °C monitored over a period of two weeks. Achiral HPLC analysis of the conversion of racemic (±)-taxifolin revealed a first-order mechanism (rate constant $k = 3.60 \times 10^{-6}$ s^{-1}, $t_{0.5} = 3210$ min; no separation of the dihydroquercetin stereoisomers; the sum of the two AUCs was set at 100%). (B) Kinetics of the enzyme-catalyzed conversion of racemic (±)-taxifolin to alphitonin at 22 °C in the presence of the partially purified enzyme (1.9 μg/mL) from *Eubacterium ramulus* (first-order rate constant $k = 7.26 \times 10^{-4}$ s^{-1}, $t_{0.5} = 16$ min; the sum of the five AUCs was set at 100%). (C) Corresponding HPLC chromatograms at 0 min (a), 30 min (b), and 60 min (c) of the enzyme-catalyzed taxifolin–alphitonin rearrangement showing the selective conversion of the (+)-taxifolin enantiomer.

Table 3. Transition States Leading from the Diketone 7 to Alphitonin (8) with One or Two Water Molecules for Proton Relay[a]

transition state	ΔG (kcal/mol)	O···C (Å)	O–H_A (Å)	O···H_B (Å)	O···C=O (deg)
1 H_2O	2.86	2.632	0.984	1.990	97.002
2 H_2O	2.34	2.533	0.979	1.904	96.767

[a]Results were obtained at the B3LYP/6-311G++(df,pd) level of theory. Geometry data and energy barriers are given in comparison to alphitonin (see Figure 5 for H_A and H_B).

EXPERIMENTAL SECTION

Standards and Materials. (±)-Taxifolin was obtained from Sigma (lot 129H1722, Steinheim, Germany). Another sample of (±)-taxifolin from Sigma (lot 015K4710) was identified as (+)-taxifolin. Solvents and reagents were of HPLC grade and obtained from J. T. Baker (Griesheim, Germany) or Sigma.

General Experimental Procedures. ^{1}H NMR spectra (500 MHz) were recorded on an Avance DRX 500 spectrometer (Bruker BioSpin, Rheinstetten, Germany), and chemical shifts δ are given in ppm referring to the signal center using the solvent peak for reference (D_2O: 4.79). IR spectra were obtained using a Bruker Tensor 27 FT-IR spectrometer. Mass spectrometry was carried out on an API 2000 mass spectrometer (Applied Biosystems, Darmstadt, Germany).

Chromatographic analyses were performed using an HPLC system consisting of a low-pressure mixing pump (model P580, Dionex, Germering, Germany) equipped with a manual injection valve (model 8125, Rheodyne, Cotati, CA, USA) having a 20 μL (analytical) or 300 μL (semipreparative) sample loop and a UV or CD detector (model UV-2075 or CD-2095, Jasco, Groß-Umstadt, Germany). Chromatograms were obtained using the Chromeleon (version 6.30, Dionex) or ChromPass (version 1.8.6.1, Jasco) chromatography software. Optimized HPLC conditions were applied as follows. Achiral separation: 250 × 10.0 mm, 7 μm, C18-silica (Polygosil 60, Macherey-Nagel, Düren, Germany), MeCN/H_2O/AcOH, 50/50/2, 5.0 mL/min, 22 °C, 273 nm. Chiral separation: 150 × 4.6 mm, 5 μm, cellulose tris(4-methylbenzoate) (OJ-RH, Daicel, Eschborn, Germany), MeCN/H_2O (pH 3, TFA), 10/90 (0 min), 10/90 (5 min), 20/80 (30 min), 70/30 (40 min), 10/90 (50 min), 0.5 mL/min, 35 °C, 273 nm. Semipreparative separation: 250 × 20.0 mm, 7 μM, C18-silica (Polygosil 60, Macherey-Nagel), MeOH/H_2O, 30/70, 5.0 mL/min, 22 °C, 220 nm.

Chiral electrokinetic chromatography was carried out on a Beckman P/ACE MDQ capillary electrophoretic system (Beckman Instruments, Fullerton, CA, USA) equipped with a photo diode array detection (DAD) system (scan range: 190–360 nm). All electropherograms were processed using the Beckman 32Karat software version 7.0. Uncoated fused-silica capillaries of 375 μm o.d. ×75 μm i.d. were obtained from Beckman and cut to 50 cm (effective length 40 cm). The following scheme was applied to wash the capillary (20 psi). Before use: 0.25 M NaOH (20 min), then H_2O (10 min); between each run: 0.25 M NaOH (3 min), then H_2O (2 min), 500 mM borate buffer pH 9 (5 min); overnight storage: 0.25 M NaOH (5 min), then H_2O (10 min) and an air stream (3 min). The capillary temperature was set to 20 °C, and the applied voltage was 18 kV. Samples were injected hydrodynamically (0.3 psi) for 3 s. Chiral separation was achieved using a 5 mM 2-hydroxypropyl-β-cyclodextrin solution in 500 mM borate buffer pH 9.

Thermal Conversion of Taxifolin and Spectroscopic Characterization of Alphitonin. (±)-Taxifolin (100 mg; Sigma, lot 129H1722) was placed in a 1 mL amber glass vial sealed with a septum screw cap, and the vial was flushed with Ar to remove O_2. Subsequently, degassed H_2O (1 mL) was added using a syringe to replace the Ar, and the vial was placed inside a 10 mL glass reactor (model TinyClave, Büchi, Flawil, Switzerland). The sample vial was submerged in degassed H_2O (10 mL), and gallic acid (1 g) was added as an external antioxidant. Finally, the glass reactor was flushed with Ar and tightly sealed. The reaction apparatus was then heated to 115 °C in an oil bath for 2 weeks, and samples were taken for in-process control. Afterward, the solution was lyophilized to obtain a crude product, of which a fraction (20.0 mg) was subjected to semipreparative HPLC to obtain (±)-alphitonin (11.2 mg) and quercetin (6.0 mg). For chiral analysis, (+)-taxifolin (1 mg; Sigma, lot 015K4710) was reacted for a time period of 60 h as described above. ^{1}H NMR (D_2O) δ 3.08 (d, 1H, ^2J(H,H) = 13.9 Hz, CH_2), 3.16 (d, 1H, ^2J(H,H) = 13.9 Hz, CH_2), 5.86 (d, 1H, ^4J(H,H) = 1.8 Hz, 5-H), 5.96 (d, 1H, ^4J(H,H) = 1.8 Hz, 7-H), 6.62 (dd, 1H, ^3J(H,H) = 8.1 Hz, ^4J(H,H) = 2.0 Hz, 6′-H), 6.70 (d, 1H, ^3J(H,H) = 8.1 Hz, 5′-H), 6.74 (d, 1H, ^4J(H,H) = 2.0 Hz, 2′-H); IR (KBr, cm^{-1}) 3422 (O–H), 1684 (C=O), 1629 (C=C); MS (ESI+) 305.3 ($[C_{15}H_{12}O_7 + H]^+$,

dx.doi.org/10.1021/np200639s | J. Nat. Prod. 2011, 74, 2243–2249

16%), 286.9 ([$C_{15}H_{12}O_7$ + H − H_2O]$^+$, 83%), 258.9 ([$C_{15}H_{12}O_7$ + H − H_2O − CO]$^+$, 100%), 230.9 ([$C_{15}H_{12}O_7$ + H − H_2O − 2 CO]$^+$, 39%); MS (ESI−) 303.3 ([$C_{15}H_{12}O_7$ − H]$^-$, 89%), 285.1 ([$C_{15}H_{12}O_7$ − H − H_2O]$^-$, 100%), 179.1 (^{5}A$^-$ and ^{2,4}B$^-$, 7%), 177.3 (^{1,4}B$^-$, 12%), 151.1 (^{2,3}A$^-$ and ^{2,3}B$^-$, 39%), 106.9 (^{1,4}A$^-$, 7%), 125.2 (^{2,4}A$^-$, 95%), 123.2 (^{5}B$^-$, 20%), 57.2 (^{6,7}B$^-$, 59%).

Enzymatic Transformation. The enzyme preparation was obtained from cultures of *Escherichia coli* heterologously expressing the taxifolin isomerase gene of *E. ramulus* (unpublished data). After disruption of *E. coli* cells by sonication and subsequent centrifugation, the resulting cell-free extract was fractionated by fast-performance liquid chromatography using a DEAE-Sephacel column according to the procedure described previously for cell extracts from *E. ramulus*.[22] A fraction with high taxifolin-transforming activity was used for the enzymatic assays. The assay contained 1165 μL of 50 mM K_3PO_4 buffer (pH 6.8) and 20 μL of the enzyme preparation (0.12 mg protein/mL) and was performed at 22 °C. The reaction was started by the addition of 65 μL of 1.2 mM (±)-taxifolin (Sigma, lot 129H1722) in DMSO. Samples (50 μL) were taken every 10 min for 100 min and immediately mixed with 50 μL of aqueous 10% MeCN acidified with TFA to pH 1. Samples were submitted directly to chromatographic analysis or were frozen using liquid nitrogen and stored at −20 °C.

Prediction of CD Spectra by Quantum Mechanical Calculations. Three-dimensional coordinates of (−)-2*R*,3*S*-epitaxifolin (**4**) and (−)-2*S*,3*S*-taxifolin (**2**) were generated and subjected to a preliminary MMFF94 force field minimization using the Chem3D software. Using the ORCA program suite,[48] a two-dimensional PES scan was carried out at the B3LYP/TZVP level of theory applying a COSMO model[49] in methanol to simulate (i) a C-ring flip leading to equatorial/axial inversion (φ_1 = C6−C7−C8−O9) and (ii) a full rotation of the B−C-ring connecting bond (φ_2 = O9−C8−C10−C11). A contour plot of the PES was prepared by a custom PERL script using GnuPlot, and minimum energy conformers were identified by visual inspection. These local minima were subjected to a free optimization at the B3LYP/TZVP level of theory again applying a COSMO methanol model, and final energies were obtained at the RI-SCS-MP2/TZVP level for accurate Boltzmann statistics. CD spectra of all local minima were then retrieved by a TDDFT/B3LYP/TZVP approach and weighted according to their individual Boltzmann population using SpecDis.

Calculations of Reaction Pathway Intermediates. Three-dimensional coordinates of all reaction pathway intermediates and of zwitterionic transition states with one or two H_2O molecules for proton relay were generated and subjected to a preliminary MMFF94 (intermediates) or MM2 (transition states) force field minimization using the Chem3D software. Using the ORCA program suite, minimum conformers of all intermediates were obtained at the B3LYP/TZVP level of theory applying a COSMO water model, followed by frequency calculations to obtain zero-point vibrational energies at 25 and 115 °C. Using the Gaussian package[38] at the B3LYP/6-311G++(df,pd) level of theory, transition states with one or two water molecules for proton relay were minimized with respect to water orientation, while the oxonium scaffold was kept frozen. In addition, structures of the diketone **7** and alphitonin (**8**) complex with one or two H_2O molecules connected by each transition state were optimized and subjected to frequency calculations. A transition-state search was carried out applying a STQN (QST3) approach at the B3LYP/6-311G++(df,pd) computational level, followed by frequency calculations to verify a single imaginary frequency and to obtain zero-point vibrational energies for subsequent estimation of the corresponding energy barrier.

AUTHOR INFORMATION

Corresponding Author

*Tel: +49-89-3168-5033. Fax: +49-89-3168-5125. E-mail: paul.elsinghorst@uni-bonn.de.

ACKNOWLEDGMENTS

The authors thank Torsten Bruhn (University of Würzburg, Germany) and Henning Henschel (Linnæus University, Sweden) for seminal support in quantum chemistry calculations of CD spectra and transition states. We gratefully acknowledge computational resources provided by the ARMINIUS cluster of the Paderborn Center for Parallel Computing (University of Paderborn, Germany). We also thank Andre Hütz (Jasco, Groß-Umstadt, Germany) for the opportunity to use the CD detector.

REFERENCES

(1) Espín, J. C.; García-Conesa, M. T.; Tomás-Barberán, F. A. *Phytochemistry* **2007**, *68*, 2986−3008.
(2) Quideau, S.; Deffieux, D.; Douat-Casassus, C.; Pouységu, L. *Angew. Chem., Int. Ed.* **2011**, *50*, 586−621.
(3) Blaut, M.; Schoefer, L.; Braune, A. *Int. J. Vitam. Nutr. Res.* **2003**, *73*, 79−87.
(4) Selma, M. V.; Espín, J. C.; Tomás-Barberán, F. A. *J. Agric. Food Chem.* **2009**, *57*, 6485−6501.
(5) Birch, A. J.; Ritchie, E.; Speake, R. N. *J. Chem. Soc.* **1960**, 3593−3599.
(6) Grover, R. K.; Maurya, R.; Roy, R. *Tetrahedron* **2004**, *60*, 2005−2010.
(7) Janes, N. F.; King, F. E.; Morgan, J. W. W. *J. Chem. Soc.* **1963**, 1356−1363.
(8) Li, X.-C.; ElSohly, H. N.; Nimrod, A. C.; Clark, A. M. *J. Nat. Prod.* **1999**, *62*, 767−769.
(9) Yoshikawa, K.; Eiko, K.; Mimura, N.; Kondo, Y.; Arihara, S. *J. Nat. Prod.* **1998**, *61*, 786−790.
(10) Volsteedt, F.; du, R.; Roux, D. G. *Tetrahedron Lett.* **1971**, *12*, 1647−1650.
(11) Li, F.; Awale, S.; Tezuka, Y.; Kadota, S. *Bioorg. Med. Chem.* **2008**, *16*, 5434−5440.
(12) Wang, Y.-F.; Cao, J.-X.; Efferth, T.; Lai, G.-F.; Luo, S.-D. *Chem. Biodiversity* **2006**, *3*, 646−653.
(13) Li, X. C.; Cai, L.; Wu, C. D. *Phytochemistry* **1997**, *46*, 97−102.
(14) Smith, H. G.; Read, J. *J. Proc. R. Soc. NSW* **1922**, *56*, 253−259.
(15) Pew, J. C. *J. Am. Chem. Soc.* **1948**, *70*, 3031−3034.
(16) Lundgren, L. N.; Theander, O. *Phytochemistry* **1988**, *27*, 829−832.
(17) Chen, K.; Ohmura, W.; Doi, S.; Aoyama, M. *Bioresour. Technol.* **2004**, *95*, 129−134.
(18) Ohmura, W.; Ohara, S.; Hashida, K.; Aoyama, M.; Doi, S. *Holzforschung* **2002**, *56*, 493−497.
(19) Gripenberg, J. *Acta Chem. Scand.* **1953**, *7*, 1323−1330.
(20) King, H. G. C.; White, T.; Hughes, R. B. *J. Chem. Soc.* **1961**, 3234−3239.
(21) Kiehlmann, E.; Li, E. P. M. *J. Nat. Prod.* **1995**, *58*, 450−455.
(22) Braune, A.; Gütschow, M.; Engst, W.; Blaut, M. *Appl. Environ. Microbiol.* **2001**, *67*, 5558−5567.
(23) Jaganath, I. B.; Mullen, W.; Lean, M. E. J.; Edwards, C. A.; Crozier, A. *Free Radical Biol. Med.* **2009**, *47*, 1180−1189.
(24) Clark-Lewis, J. W.; Korytnyk, W. *J. Chem. Soc.* **1958**, 2367−2372.
(25) Gaffield, W. *Tetrahedron* **1970**, *26*, 4093−4108.
(26) Gaffield, W.; Waiss, A. C.; Tominaga, T. *J. Org. Chem.* **1975**, *40*, 1057−1061.
(27) Mehta, P. P.; Whalley, W. B. *J. Chem. Soc.* **1963**, 5327−5332.
(28) Nonaka, G.-I.; Goto, Y.; Kinjo, J.-E.; Nohara, T.; Nishioka, I. *Chem. Pharm. Bull.* **1987**, *35*, 1105−1108.
(29) Sakushima, A.; Nishibe, S. *Phytochemistry* **1988**, *27*, 948−950.
(30) Snatzke, G. *Tetrahedron* **1965**, *21*, 413−419.
(31) Snatzke, G. *Tetrahedron* **1965**, *21*, 439−448.
(32) Zenkevich, I. G.; Makarov, V. G.; Eshchenko, A. Y. *Rastitel'nye Resursy* **2006**, *42*, 81−92.
(33) Markham, K. R.; Mabry, T. J. *Tetrahedron* **1968**, *24*, 823−827.

(34) Bringmann, G.; Bruhn, T.; Maksimenka, K.; Hemberger, Y. *Eur. J. Org. Chem.* **2009**, 2717−2727.
(35) Gaffield, W. *Chem. Pharm. Bull.* **1996**, *44*, 1102−1103.
(36) Faizi, S.; Siddiqi, H.; Naz, A.; Bano, S.; Lubna. *Helv. Chim. Acta* **2010**, *93*, 466−481.
(37) Volsteedt, F.; du, R.; Rall, G. J. H.; Roux, D. G. *Tetrahedron Lett.* **1973**, *14*, 1001−1004.
(38) Frisch, M. J.; Trucks, G. W.; Schlegel, H. B.; Scuseria, G. E.; Robb, M. A.; Cheeseman, J. R.; Montgomery, J.; Vreven, T.; Kudin, K. N.; Burant, J. C.; Millam, J. M.; Iyengar, S. S.; Tomasi, J.; Barone, V.; Mennucci, B.; Cossi, M.; Scalmani, G.; Rega, N.; Petersson, G. A.; Nakatsuji, H.; Hada, M.; Ehara, M.; Toyota, K.; Fukuda, R.; Hasegawa, J.; Ishida, M.; Nakajima, T.; Honda, Y.; Kitao, O.; Nakai, H.; Klene, M.; Li, X.; Knox, J. E.; Hratchian, H. P.; Cross, J. B.; Bakken, V.; Adamo, C.; Jaramillo, J.; Gomperts, R.; Stratmann, R. E.; Yazyev, O.; Austin, A. J.; Cammi, R.; Pomelli, C.; Ochterski, J. W.; Ayala, P. Y.; Morokuma, K.; Voth, G. A.; Salvador, P.; Dannenberg, J. J.; Zakrzewski, V. G.; Dapprich, S.; Daniels, A. D.; Strain, M. C.; Farkas, O.; Malick, D. K.; Rabuck, A. D.; Raghavachari, K.; Foresman, J. B.; Ortiz, J. V.; Cui, Q.; Baboul, A. G.; Clifford, S.; Cioslowski, J.; Stefanov, B. B.; Liu, G.; Liashenko, A.; Piskorz, P.; Komaromi, I.; Martin, R. L.; Fox, D. J.; Keith, T.; Al-Laham, M. A.; Peng, C. Y.; Nanayakkara, A.; Challacombe, M.; Gill, P. M. W.; Johnson, B.; Chen, W.; Wong, M. W.; Gonzalez, C.; Pople, J. A. *Gaussian 03*; Gaussian, Inc.: Wallingford, CT, USA, 2004.
(39) Henschel, H.; Karlsson, B. C. G.; Rosengren, A. M.; Nicholls, I. A. *J. Mol. Struct. (Theochem)* **2010**, *958*, 7−9.
(40) Bekker, R.; Li, X. C.; ElSohly, H. N.; Clark, A. M.; Brandt, E. V.; Ferreira, D. *J. Nat. Prod.* **2001**, *64*, 345−347.
(41) Bekker, R.; Brandt, E.; Ferreira, D. *Tetrahedron Lett.* **1998**, *39*, 6407−6410.
(42) Bekker, R.; Brandt, E. V.; Ferreira, D. *Chem. Commun.* **1996**, 957−958.
(43) Boumendjel, A.; Macalou, S.; Valdameri, G.; Pozza, A.; Gauthier, C.; Arnaud, O.; Nicolle, E.; Magnard, S.; Falson, P.; Terreux, R.; Carrupt, P.-A.; Payen, L.; Di Pietro, A. *Curr. Med. Chem.* **2011**, *18*, 3387−3401.
(44) Boumendjel, A. *Curr. Med. Chem.* **2003**, *10*, 2621−2630.
(45) Haudecoeur, R.; Ahmed-Belkacem, A.; Yi, W.; Fortuné, A.; Brillet, R.; Belle, C.; Nicolle, E.; Pallier, C.; Pawlotsky, J.-M.; Boumendjel, A. *J. Med. Chem.* **2011**, *54*, 5395−5402.
(46) Lee, C.-Y.; Chew, E.-H.; Go, M.-L. *Eur. J. Med. Chem.* **2010**, *45*, 2957−2971.
(47) Thuy, T. T.; Kamperdick, C.; Ninh, P. T.; Lien, T. P.; Thao, T. T. P.; Sung, T. V. *Pharmazie* **2004**, *59*, 297−300.
(48) Neese, F. *ORCA−An ab Initio, Density Functional and Semiempirical Program Package*; University of Bonn: Bonn, Germany, 2011.
(49) Sinnecker, S.; Rajendran, A.; Klamt, A.; Diedenhofen, M.; Neese, F. *J. Phys. Chem. A* **2006**, *110*, 2235−2245.